A&A 430, L33–L36 (2005)
DOI: 10.1051/0004-6361:200400124

Astronomy & Astrophysics

Letter to the Editor

X-ray tomography of a cometary bow shock

R. Wegmann[1] and K. Dennerl[2]

[1] Max-Planck-Institut für Astrophysik, 85748 Garching, Germany
e-mail: ruw@mpa-garching.mpg.de
[2] Max-Planck-Institut für extraterrestrische Physik, 85748 Garching, Germany
e-mail: kod@mpe.mpg.de

Received 24 November 2004 / Accepted 11 December 2004

Abstract. The volume intensity of the cometary X-ray emission is enhanced behind the bow shock by a factor of up to three. This effect offers the opportunity to identify the bow shock by a tomographic method in X-ray images of comets. By an analysis of the X-ray data obtained by XMM-Newton from Comet C/2000 WM1 (LINEAR) we obtain information on the position, the shape and the structure of the bow shock of this comet. In particular, we get for the first time a global image of the subsolar part of the bow shock, which up to now has not been visited by spacecrafts. The shock is not a sharp discontinuous jump but rather a gradual transition in a region of about 40 000 km width. An asymmetry can well be explained by the inclination of the interplanetary magnetic field. Our results are consistent with theoretical expectations as well as with results from spacecraft observations.

Key words. comets: general – shock wave – X-rays: comets

1. Introduction

When a comet passes through the inner solar system, gas sublimates from the surface of the nucleus and forms a huge cloud. The molecules and atoms in this cloud are ionized by various processes and picked up by the solar wind. The solar wind can only digest a certain amount of additional mass. Then the supersonic parallel flow must turn into a subsonic divergent flow. A bow shock must form.

This theoretical prediction was developed and first studied by one-dimensional hydrodynamic model calculations by Biermann et al. (1967). Refined hydrodynamic and magnetohydrodynamic model calculations in two and three dimensions predicted a weak shock of Mach number about 2 (Schmidt & Wegmann 1982). On the other hand doubts remained whether a cometary bow shock really exists (Wallis & Dryer 1985).

First in situ observations became available with the spacecraft missions to the comets Giacobini-Zinner and Halley. Interpretation of the results was not straightforward. Observers came finally to the conclusion that a bow shock was really observed at comet Giacobini-Zinner by the ICE spacecraft (Smith et al. 1986). The interpretation of the data as a bow shock was supported by the fact that measured flow values upstream and somewhere downstream are connected by the Rankine-Hugoniot conditions.

The bow shock at comet Halley was detected by the Giotto spacecraft (Coates et al. 1987), the Vega 1 and Vega 2 spacecrafts (Galeev et al. 1986) and (arguably) by the Suisei spacecraft (Mukai et al. 1986). Also in the encounters of Giotto with comet Grigg-Skjellerup (Johnstone et al. 1993) and of Deep Space 1 with comet Borrelly (Young et al. 2004) shock features were detected. With only one possible exception (Giotto on the outbound path through comet Grigg-Skjellerup) the shock is not marked by a discontinuous change in the flow variables but by a transition zone of about 40 000 km width. The width was as large as 120 000 km in the quasi-parallel shock at comet Halley on the Giotto outbound pass (Neubauer et al. 1990). Coates (1995) reviews the observations by six spacecrafts of the bow shocks at three comets.

Spacecraft encounters with comets give plasma parameters along a one-dimensional line. The passage through the shock typically occurs at the flanks, where the shock is expected to be weaker than in the subsolar region. The shock may even have decayed to a bow wave. Measurements near the shock are disturbed by the heavy turbulence generated by the ion pick-up and by the shock. The onset of turbulence has even been used as a shock indicator (Galeev et al. 1986). The subsolar shock distance is estimated by fitting a suitable parabola to the data on the flanks.

We show in this paper how further evidence for and information about a cometary bow shock can be obtained from X-ray observations. The X-ray photons are collected from the distance and so render a more global view onto the comet. This admits the reconstruction of the bow shock in three dimensions over a wide range on the subsolar side. The results of our analysis confirm the theoretical predictions of shock position and shape. The shock, however, is not a sharp jump but rather a transition region of about 40 000 km width where the flow

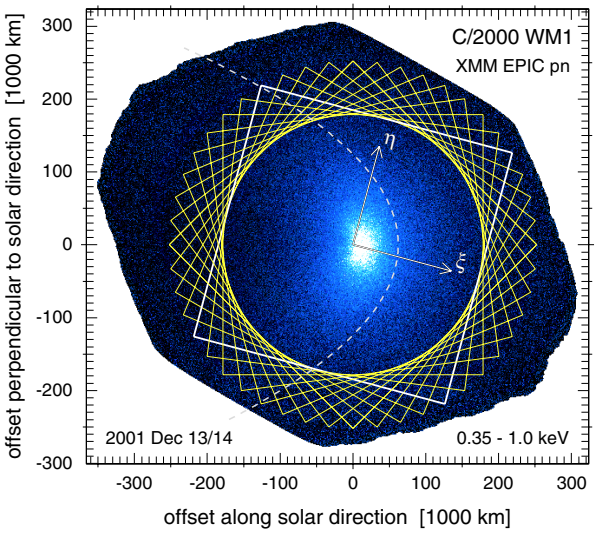

Fig. 1. X-ray image of Comet C/2000 WM1, binned into 4″×4″ pixels and displayed in a linear intensity scale, ranging from 0.0 (black) to 0.25 counts s^{-1} $arcmin^{-2}$ (white). The coordinate system is centered on the cometary nucleus, and the positive x axis is oriented towards the Sun. Tilted squares mark the areas used for the analysis described in the text. They are all completely inside the displayed field of view, which shows the area which received an effective exposure of at least 5000 s. The coordinate system (ξ, η) is illustrated for the square which is tilted by $\alpha = -15°$. The dashed line marks the predicted position of the bow shock.

variables change approximately linearly. The inclination of the interplanetary magnetic field imposes an asymmetry.

2. Observable effects of the bow shock on the X-ray emission

It has been shown by model calculations (Wegmann et al. 2004) that the volume intensity of the cometary X-ray emission changes in the shock discontinuously by a factor of up to three.

We use a coordinate system x, y, z, centered at the comet, with x along the Sun-Comet line, positive towards the Sun, and with the z-axis parallel to the line of sight. The observed data are surface intensities $J(x, y)$ [erg cm^{-2} s^{-1}], i.e., volume intensities $I(x, y, z)$ integrated over the z coordinate as line of sight. The data for the surface intensity $J(x, y)$ are given in a certain region with irregular boundary (see Fig. 1). We study the data in a square R_α with sides of length $2a$, rotated by an angle α in the counterclockwise direction. We introduce in the square auxiliary coordinates ξ, η obtained from x, y by rotation by the angle α (see Fig. 1). In the square R_α we consider the surface intensity as function $J(\xi, \eta)$ of the new coordinates.

We calculate for a fixed angle α the averages

$$A(\xi) = \frac{1}{2a} \int_{-a}^{a} J(\xi, \eta) \mathrm{d}\eta \tag{1}$$

of the surface intensity $J(\xi, \eta)$ in the square R_α on the lines ξ = const.

We study two cases:

Case 1: **Jump**. We assume first that at the shock surface S, the volume intensity I changes discontinuously by an amount ΔI. Elementary differential geometry shows that at the position ξ_S where the line ξ = const. touches (i.e. becomes tangent to) the shock, the derivative $A' = \mathrm{d}A/\mathrm{d}\xi$ is discontinuous. It jumps by the amount

$$\Delta A' = \frac{\pi R_K \cos\alpha}{a} \Delta I \tag{2}$$

where the radius of curvature R_K is defined by $R_K = 1/\sqrt{K}$ in terms of the Gaussian curvature K of the shock surface S at the tangent point.

Case 2: **Linear transition**. We assume that this transition happens in a spherical shell with outer radius R_K and inner radius $R_i < R_K$. We assume further that the volume intensity increases in the shell linearly by an amount ΔI which is reached at the inner sphere. The "shock width" is then defined as $\Delta\xi = \xi_S - \xi_i = R_K - R_i$. An elementary calculation shows that A' is proportional to $\xi(R_K - \xi)$ in the interval $\xi_i < \xi < \xi_S$. If $\Delta\xi$ is small compared to R_K, the derivative A' has a (nearly) linear part in the interval $\xi_i < \xi < \xi_S$. The total change of the derivative in this interval is

$$\Delta A' = \frac{\pi R_i \cos\alpha}{a} \Delta I. \tag{3}$$

This shows that the total change of A' in a linear transition is by the fraction $\Delta\xi/R_K$ less than the change (2) in a jump.

Model calculations show that the bow shock is well approximated in the subsolar region by a paraboloid

$$x = R_S - \frac{y^2 + z^2}{4R_S} \tag{4}$$

where R_S is the subsolar bow shock distance. At the point where a plane $\xi = \xi_S$ = const., inclined by an angle α with respect to the y axis, touches the shock surface, the radius of curvature is

$$R_K = \frac{2R_S}{\cos^2\alpha}. \tag{5}$$

3. Data analysis

We analyze observations of comet C/2000 WM1 (LINEAR) obtained on Dec. 13/14, 2001 with XMM-Newton (Dennerl et al. 2003). Figure 1 shows the observed surface intensities. We use squares with sides of length $2a$ = 358 000 km. Wegmann et al. (2004) have determined the subsolar distance R_S = 62 000 km of the bow shock. (Wegmann et al. (2004) used for their analysis a pixel size of 5″ instead of the correct 4″. Therefore, their length scales all have to be reduced by the factor 0.8). The shock parabola defined by Eq. (4) has been inserted into Fig. 1. Figure 14 of the paper of Wegmann et al. (2004) shows the X-ray intensities from the observation and from a model. The top panels of this figure show the averages $A(\xi)$ for the angles $\alpha = 0°$ and $\alpha = 90°$.

We have calculated the derivatives A' for thirteen angles between −45° and +45° in steps of 7.5°, i.e., for all the squares

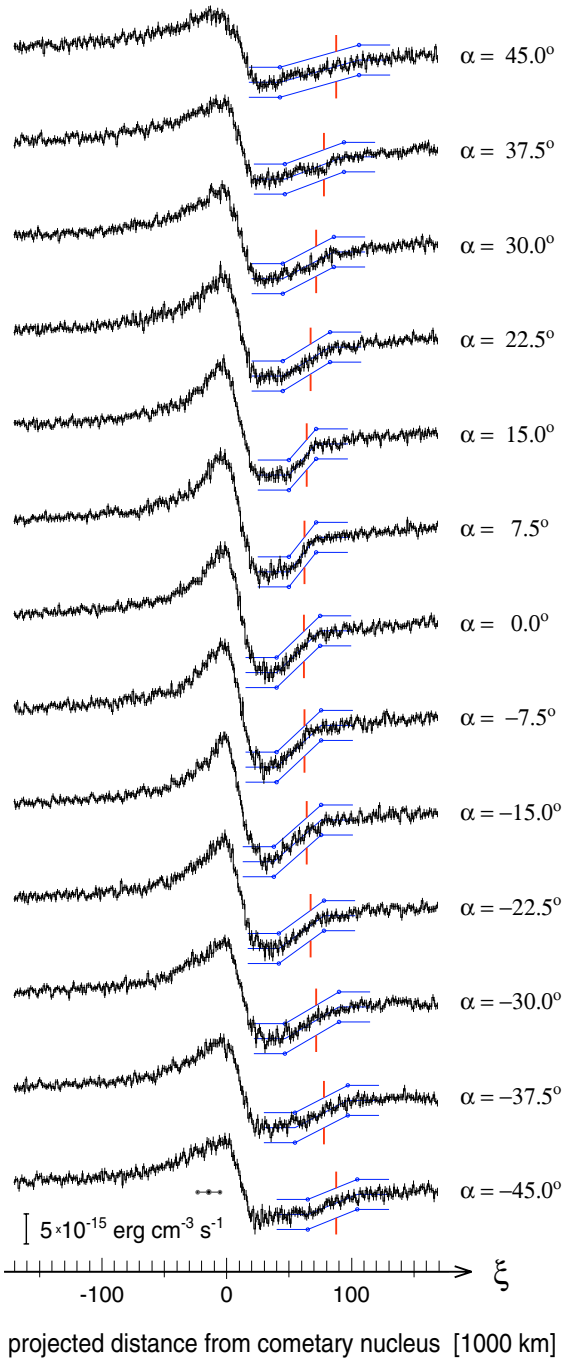

Fig. 2. The derivative $A'(\xi)$ for the 13 angles α indicated at right. It was approximated by $A'(\xi_i) \sim (A(\xi_{i+7}) - A(\xi_{i-7}))/14\Delta\xi$, for each $\Delta\xi = 4''$ (=1190 km) wide bin ξ_i (the small illustration at bottom shows the size of $14\Delta\xi$). The 1σ errors for $A'(\xi_i)$ are marked for each bin. Exposure variations were taken into account in the calculation of $A(\xi_i)$. Vertical lines mark the theoretical position of the bow shock. The derivatives near the shock are approximated by a piecewise linear function, which indicates the linear behaviour near the shock and its lower and upper limits. For better clarity, this function is repeated above and below each derivative.

shown in Fig. 1. The derivative A' is approximated by the difference quotient over 14 pixels. The result is shown in Fig. 2. For all angles there is a clearly recognizable, distinct linearly increasing part in an interval $\xi_1 \le \xi \le \xi_2$. We have determined

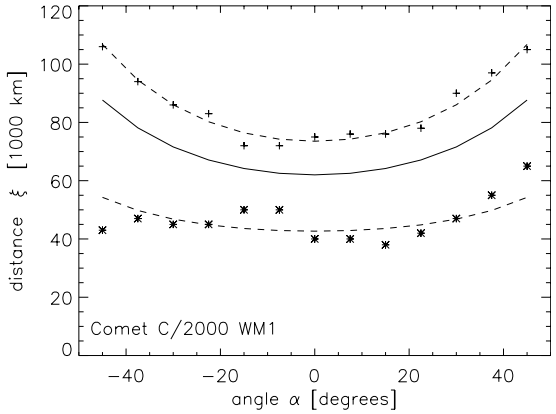

Fig. 3. The boundary points ξ_1 (stars), and ξ_2 (plus) of the linear part of the function $A'(\xi)$ determined from Fig. 2 plotted as function of the angle α. The dashed lines are least square fits of paraboloidal shapes. The solid curve is for the theoretical shock parabola.

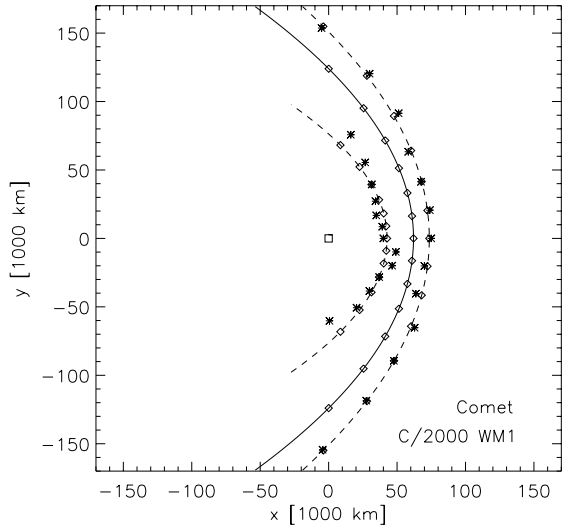

Fig. 4. The theoretical shock (solid line), the parabolas approximating the boundaries of the shock region (dashed) and for thirteen angles the tangent points (diamonds) to the parabolas for these angles. The numerically determined distances of the shock boundaries are marked by stars. The square marks the position of the nucleus.

the points ξ_1, ξ_2 by fitting a line to the numerical derivatives shown in Fig. 2 in the ξ interval where the derivative obviously increases linearly. This gives the distances to the nucleus of the tangents at the inner and outer boundaries of the shock transition region.

In Fig. 3 we have plotted the distances ξ_1 and ξ_2 of the inner and outer ends of the linear part of A' as a function of α. We have determined least squares approximations by linear combinations of the functions $f_1(\alpha) := \cos\alpha$ and $f_2(\alpha) := \sin\alpha\tan\alpha$. This corresponds to paraboloidal shapes of the boundary curves. The fit for the outer boundary is rather good. The inner boundary is less well represented. The curve for the theoretical shock parabola lies in between.

We have entered in Fig. 4 the theoretical shock parabola and the parabolas fitted to the outer and inner boundaries of the shock region as shown in Fig. 3. The numerically determined points are close to these parabolas.

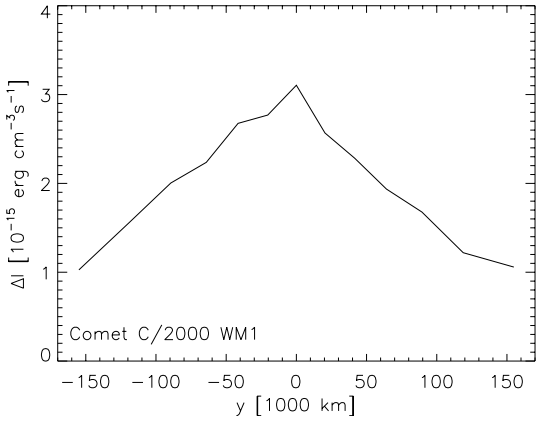

Fig. 5. The change ΔI of the volume intensity in the shock transition as a function of the coordinate y of the outer parabola.

We can finally use formula (3) to determine from the change of A' in the shock region the change of the intensity

$$\Delta I = \frac{a\,\Delta A'}{\pi R_K \cos\alpha\,(1 - \Delta\xi/R_K)} \tag{6}$$

in the shock transition. We use the radius of curvature R_K of the parabola fitted to the outer points ξ_2 (see Fig. 4) and as $\Delta A'$ the difference between the horizontal lines in the graphs of A' shown in Fig. 2. The increase in intensity during the shock transition calculated by this method as a function of the y-coordinate of the outer parabola is shown in Fig. 5.

4. Effect of the interplanetary magnetic field

The volume intensity of the X-ray emission is given by

$$I = N_i N_\mathrm{n} v_\mathrm{eff} Q E \tag{7}$$

with the heavy ion density N_i, the neutral density N_n, the cross-section Q for charge exchange, the average energy E emitted in a charge exchange interaction and the effective velocity v_eff, which is a combination of the flow velocity v_flow and the thermal velocity v_therm. Only N_i and v change in the shock. The product $N_i v_\mathrm{flow}$ remains constant. The thermal velocity, however, increases in the shock due to the shock heating. The fact, that the intensity I changes not discontinuously but gradually in the shock, seems to indicate that the transformation of the flow speed into thermal speed takes time.

The gyration period of a water ion H_2O^+ in a magnetic field of $B = 10$ nT is about 120 s. The measured cometary ion pressure completely dominates the shock region (Coates 1995). The width of the shock region of around 40 000 km can be interpreted in the way that the ions need a few (about 3–4) full gyrations to transform the kinetic energy into thermal energy and to build up the high pressure behind the shock.

The change in intensity during the shock transition shown in Fig. 5 is asymmetric. It is larger for negative y than for positive y. This asymmetry can be explained by the inclination of the interplanetary magnetic field. When the field has a positive angle α of inclination, the shock is quasi-perpendicular for positive y and quasi-parallel for negative y. In a quasi-perpendicular shock the field is compressed and contributes to the increased total pressure. The gas pressure is low. Hence the thermal velocity and the X-ray intensity are low. In a quasi-parallel shock, the field strength remains nearly constant. The ion pressure must be higher on this side. The thermal velocity and the X-ray intensity are higher. This explains the asymmetry of Fig. 5.

The gyration period behind the quasi-parallel shock is larger than behind the quasi-perpendicular shock. If the shock width is always about three gyration periods times velocity, the shock width must be larger for a quasi-parallel shock. Therefore, the same field inclination used for the explanation of the asymmetry in ΔI can explain, why the width of the shock in Fig. 4 seems to be larger for negative y than for positive y. The extraordinarily large width of 120 000 km of the quasi-parallel shock found on the Giotto outbound pass through comet Halley (Neubauer et al. 1990) fits nicely to this result.

5. Conclusions

The cometary bow shock leaves traces in X-ray data. These traces can be identified in the derivatives of averages along straight lines. The data for comet WM1 are good enough such that the derivatives can be calculated as sufficiently smooth functions.

We obtain by a tomographic method information about a rather extended section of the subsolar part of the bow shock of Comet C/2000 WM1 (LINEAR). It turns out that the shock is not discontinuous, but an approximately linear transition of the flow variables from the unshocked to the shocked state. The width of the shock region seems to be about three gyration periods multiplied by flow velocity. An asymmetry in the shape of the bow shock and in the change in X-ray intensity can be explained by the effect of the inclination of the interplanetary magnetic field.

References

Biermann, L., Brosowski, B., & Schmidt, H. U. 1967, Sol. Phys., 1, 254
Coates, A. J., Johnstone, A. D., Thomsen, M. F., et al. 1987, A&A, 187, 55
Coates, A. J. 1995, Adv. Space Res., 15, 403
Dennerl, K., Aschenbach, B., Burwitz, V., et al. 2003, in X-Ray and Gamma-Ray telescopes and instruments in astronomy, ed. J. E. Trümper, & H. D. Tananbaum, Proc. SPIE, 4851, 277
Galeev, A. A., Gribov, B. E., Gombosi, T., et al. 1986, Geophys. Res. Lett., 13, 841
Johnstone, A. D., Coates, A. J., Huddleston, D. E., et al. 1993, A&A, 273, L1
Mukai, T., Miyake, W., Terasawa, T., et al. 1986, Nature, 321, 299
Neubauer, F. M., Glassmeier, K. H., Akuña, M. H., et al. 1990, Ann. Geophys., 8, 463
Schmidt, H. U., & Wegmann, R. 1982, in Comets, ed. L. L. Wilkening (Tucson: Univ. Arizona Press), 538
Smith, E. J., Slavin, J. A., Bame, S. J., et al. 1986, ESA-SP 250, Vol. 3, 461
Wallis, M. K., & Dryer, M. 1985, Nature, 318, 646
Wegmann, R., Dennerl, K., & Lisse, C. M. 2004, A&A, 428, 647
Young, D. T., Crary, F. J., Nordholt, J. E., et al. 2004, Icarus, 167, 80